

Supporting Information

**Improvement effect of *p*-sulfonatocalix[4]arene on the performance of PEG/salt
aqueous two-phase system**

Yanrong Cheng, Wenlin Xu, Yaqiong Wang, Xia Guo*

School of Chemistry and Chemical Engineering, Yangzhou University, Yangzhou, Jiangsu, 225002,
P. R. China

Figure Captions

Fig. S1 Panel A shows the UV–Vis absorption spectra of different concentrations of SC[4], and Panel B shows the calibration curve of SC[4]. Panels C and D are the UV–Vis absorption spectra of the bottom phases of PEG 600 (25.0 wt%)/(NH₄)₂SO₄ (20.0 wt%)/SC[4] (5.0 wt%) and PEG 600 (25.0 wt%)/(NH₄)₂SO₄ (20.0 wt%)/SC[4] (3.0 wt%)/[C₁₂mim]Br (3.0 wt%) ATPSs.

Fig. S2 The UV–Vis absorption spectra of standard solutions of [C_nmim]Br (Panels A, D, and G) and the calibration curves of [C_nmim]Br (Panels B, E, and H). Panels C, F, and I present the UV–Vis absorption spectra of the bottom phases of PEG 600/(NH₄)₂SO₄/SC[4]/[C_nmim]Br ATPS. To make the samples suitable for UV-detection, the bottom phase in Panel C was diluted 800 times, and in Panels F and I, the bottom phase was diluted 3200 times.

Fig. S3 Panels A, C, and E are the UV–Vis absorption spectra of the standard solutions of MA, Trp, and Phe, and Panels B, D, and F give the calibration curves for MA, Phe, and Trp, respectively. Panels G, H, and I are the UV–Vis absorption spectra of the bottom phases of the PEG 600 (25.0 wt%)/(NH₄)₂SO₄ (20.0 wt%)/SC[4] (3.0 wt%)/[C₁₂mim]Br (2.0 wt%) ATPS including MA, Trp, and Phe, respectively. The bottom phases of the ATPSs without MA, Trp, and Phe were used as the blank in the UV-detection (Panels A, C, E, G, H, and I), and also used as the solvent in the determination of calibration curves (Panels A, C, and E). When measuring Phe absorbance, the bottom phase was diluted 4 times.

Fig. S4 Panels A and B show the HPLC chromatogram and the peak areas of the standard solutions of Phe, and Panel C gives the calibration curve for Phe concentration versus HPLC peak area. Panel D is the HPLC chromatogram for the triple diluted top phase of the PEG 600 (25.0 wt%)/(NH₄)₂SO₄ (20.0 wt%)/SC[4] (0.1 wt%)/[C₁₂mim]Br (5.0 wt%)/Phe ATPS. These HPLC experiments were carried out on an HPLC (LC-20A, Shimadzu, Japan) system using a reverse phase column. Methanol/ultrapure water (3:6, v/v) solution was used as the mobile phase.

Fig. S5 The ^1H NMR spectra of the top phase of PEG 600 (25.0 wt%)/(NH_4)₂SO₄ (20.0 wt%) ATPS in the absence (a) and presence of an adjuvant (b-d). Adjuvant: SC[4] (1.0 wt%, b), [C₆mim]Br (5.0 wt%, c), and SC[4] (1.0 wt%)/[C₆mim]Br (5.0 wt%) (d).

Fig. S6 The ^1H NMR spectra of the top phase of PEG 600 (25.0 wt%)/(NH_4)₂SO₄ (20.0 wt%)/MA ATPS in the absence (a) and presence (b-d) of an adjuvant. Adjuvant: SC[4] (1.0 wt%, b), [C₆mim]Br (5.0 wt%, c), and SC[4] (1.0 wt%)/[C₆mim]Br (5.0 wt%) (d).

Fig. S7 The partition coefficients of MA (K_{MA}), Trp (K_{Trp}), and Phe (K_{Phe}) in PEG 600/(NH_4)₂SO₄/SC[4] (1.0 wt%)/[C_nmim]Br (5.0 wt%) ATPS at different pH values.

Fig. S8 The partition coefficients of MA, Trp, and Phe in PEG 600/(NH_4)₂SO₄/SC[4]/[C_nmim]Br ATPS at pH 7. The total weight of [C_nmim]Br + SC[4] is 5.0 wt%.

Fig. S9 Effect of pH on the partition coefficients of SC[4] (5.0 wt%) in PEG 600 (25.0 wt%)/(NH_4)₂SO₄ (20.0 wt%)/SC[4] (5.0 wt%) ATPS.

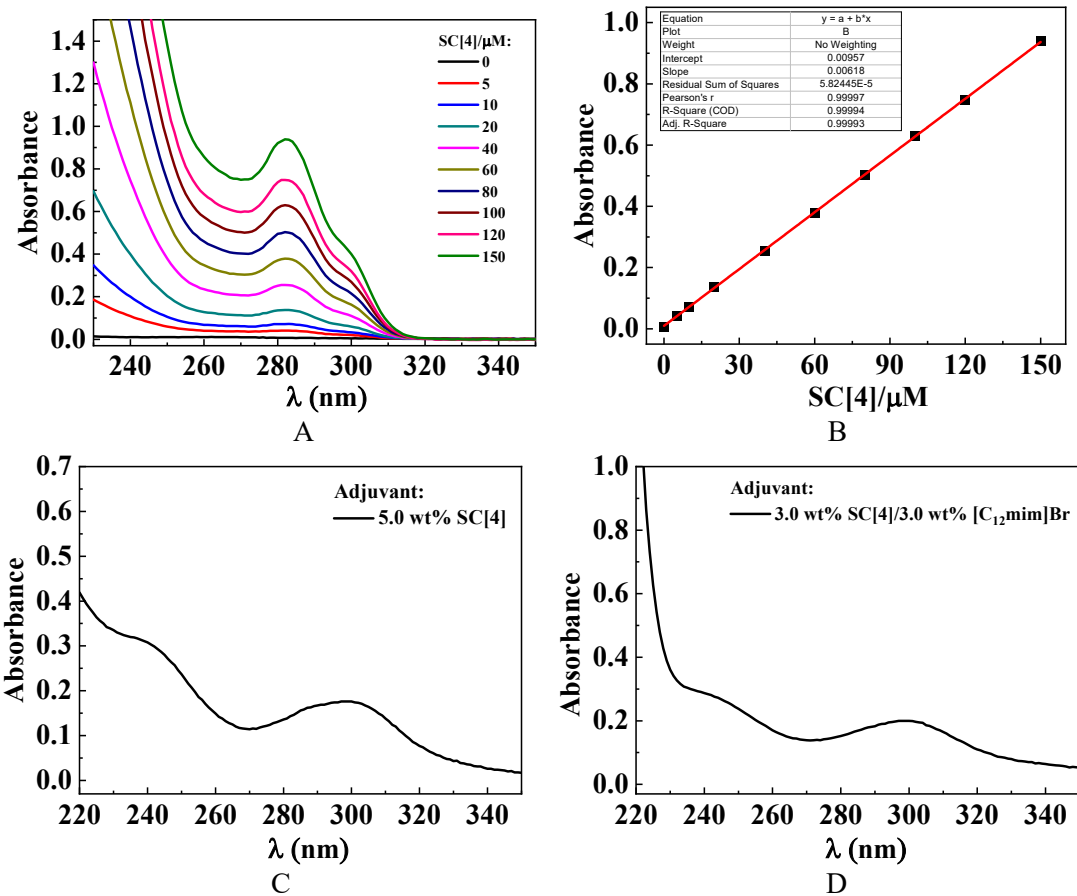


Fig. S1 Panel A shows the UV–Vis absorption spectra of different concentrations of SC[4], and Panel B shows the calibration curve of SC[4]. Panels C and D are the UV–Vis absorption spectra of the bottom phases of PEG 600 (25.0 wt%)/(NH₄)₂SO₄ (20.0 wt%)/SC[4] (5.0 wt%) and PEG 600 (25.0 wt%)/(NH₄)₂SO₄ (20.0 wt%)/SC[4] (3.0 wt%)/[C₁₂mim]Br (3.0 wt%) ATPSs.

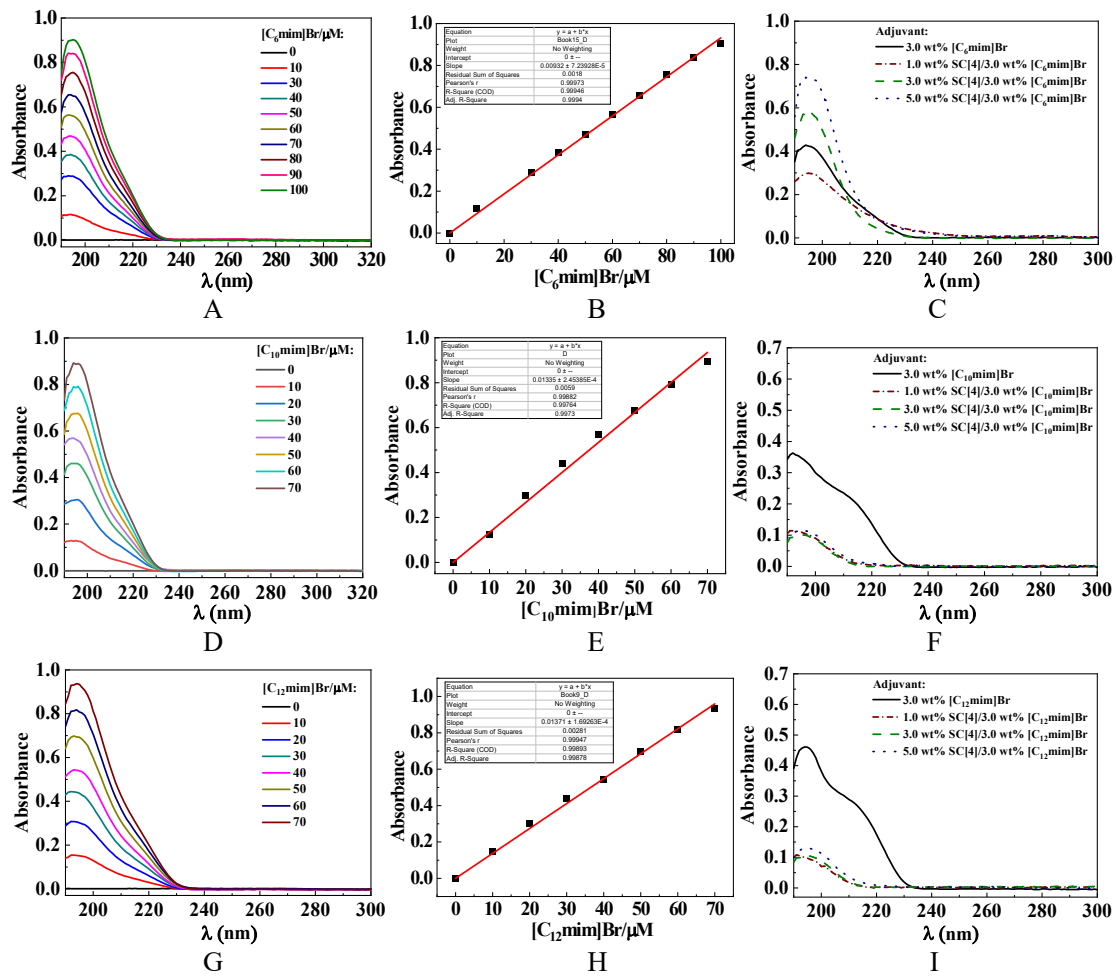


Fig. S2 The UV–Vis absorption spectra of standard solutions of $[C_n\text{mim}]Br$ (Panels A, D, and G) and the calibration curves of $[C_n\text{mim}]Br$ (Panels B, E, and H). Panels C, F, and I present the UV–Vis absorption spectra of the bottom phases of PEG 600/ $(\text{NH}_4)_2\text{SO}_4$ /SC[4]/ $[C_n\text{mim}]Br$ ATPS. To make the samples suitable for UV-detection, the bottom phase in Panel C was diluted 800 times, and in Panels F and I, the bottom phase was diluted 3200 times.

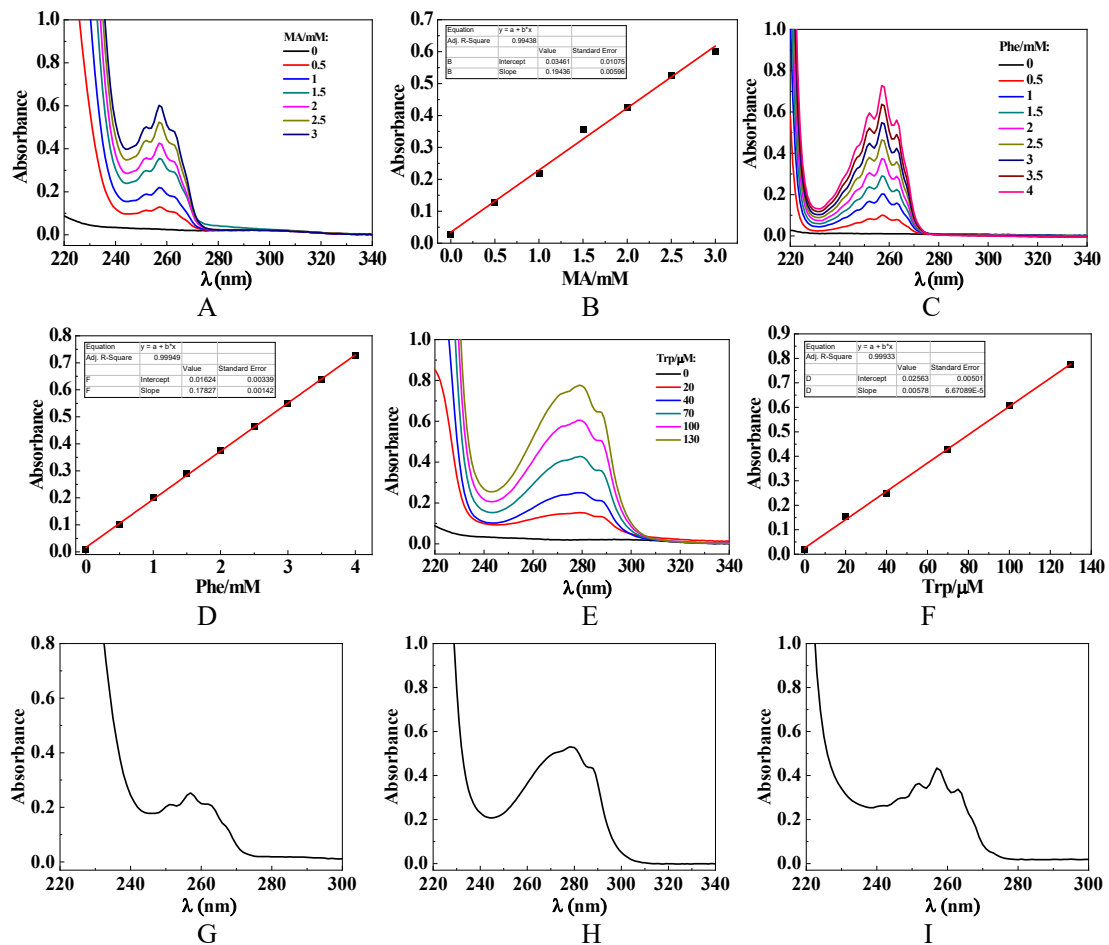


Fig. S3 Panels A, C, and E are the UV–Vis absorption spectra of the standard solutions of MA, Trp, and Phe, and Panels B, D, and F give the calibration curves for MA, Phe, and Trp, respectively. Panels G, H, and I are the UV–Vis absorption spectra of the bottom phases of the PEG 600 (25.0 wt%)/(NH₄)₂SO₄ (20.0 wt%)/SC[4] (3.0 wt%)/[C₁₂mim]Br (2.0 wt%) ATPS including MA, Trp, and Phe, respectively. The bottom phases of the ATPSs without MA, Trp, and Phe were used as the blank in the UV-detection (Panels A, C, E, G, H, and I), and also used as the solvent in the determination of calibration curves (Panels A, C, and E). When measuring Phe absorbance, the bottom phase was diluted 4 times.

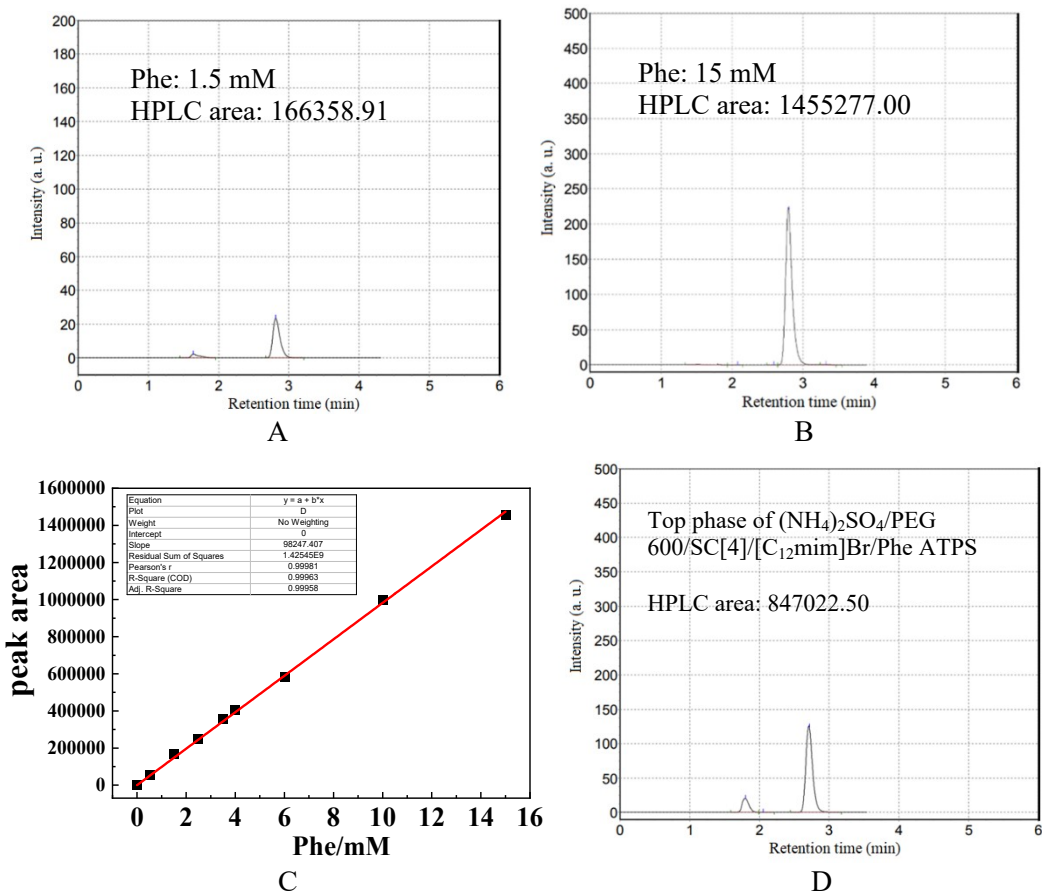


Fig. S4 Panels A and B show the HPLC chromatogram and the peak areas of the standard solutions of Phe, and Panel C gives the calibration curve for Phe concentration versus HPLC peak area. Panel D is the HPLC chromatogram for the triple diluted top phase of the PEG 600 (25.0 wt%)/($\text{NH}_4)_2\text{SO}_4$ (20.0 wt%)/SC[4] (0.1 wt%)/[C₁₂mim]Br (5.0 wt%)/Phe ATPS. These HPLC experiments were carried out on an HPLC (LC-20A, Shimadzu, Japan) system using a reverse phase column. Methanol/ultrapure water (3:6, v/v) solution was used as the mobile phase.

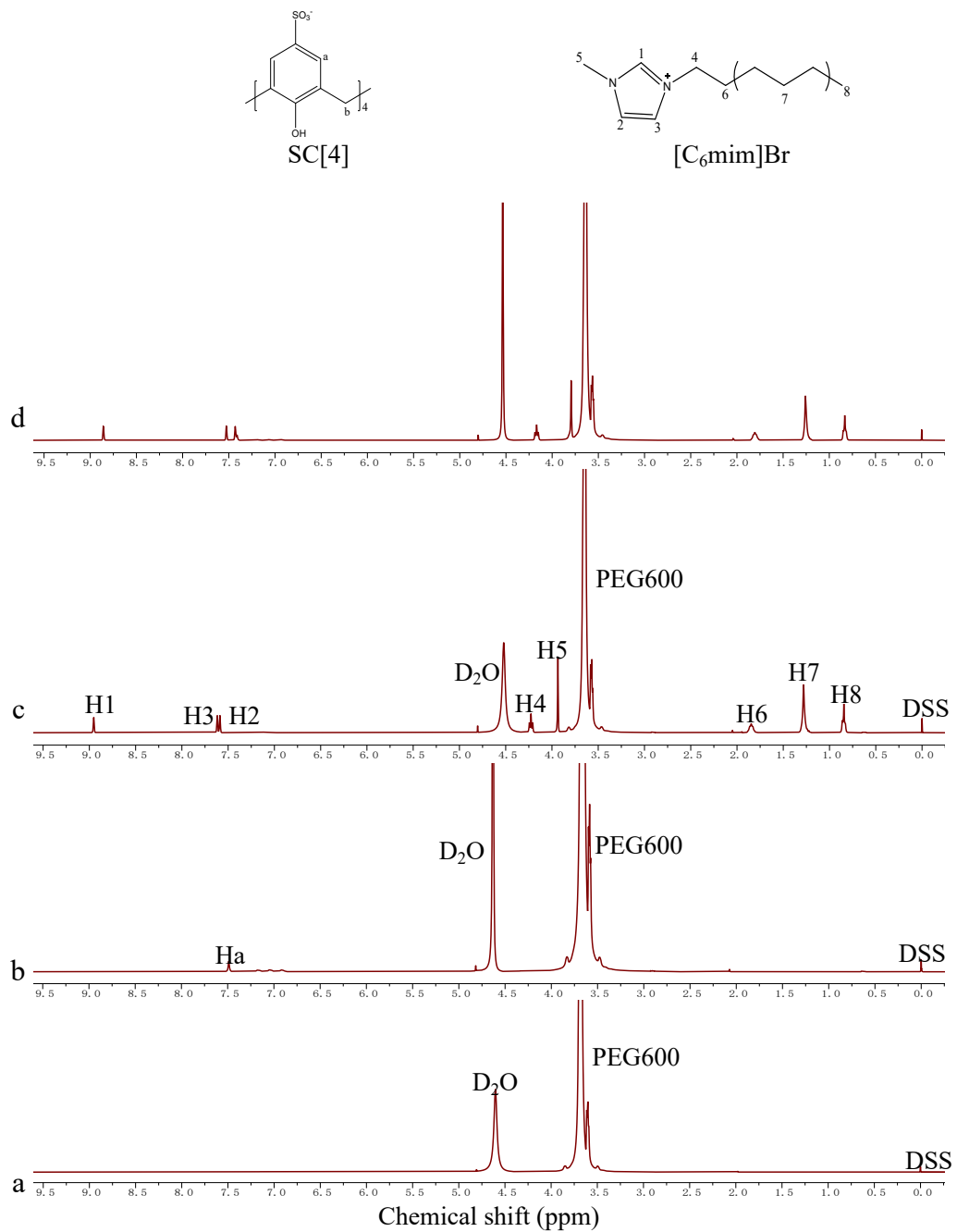


Fig. S5 The ^1H NMR spectra of the top phase of PEG 600 (25.0 wt%)/($\text{NH}_4\text{}_2\text{SO}_4$ (20.0 wt%) ATPS in the absence (a) and presence of an adjuvant (b-d). Adjuvant: SC[4] (1.0 wt%, b), $[\text{C}_6\text{mim}] \text{Br}$ (5.0 wt%, c), and SC[4] (1.0 wt%)/ $[\text{C}_6\text{mim}] \text{Br}$ (5.0 wt%) (d).

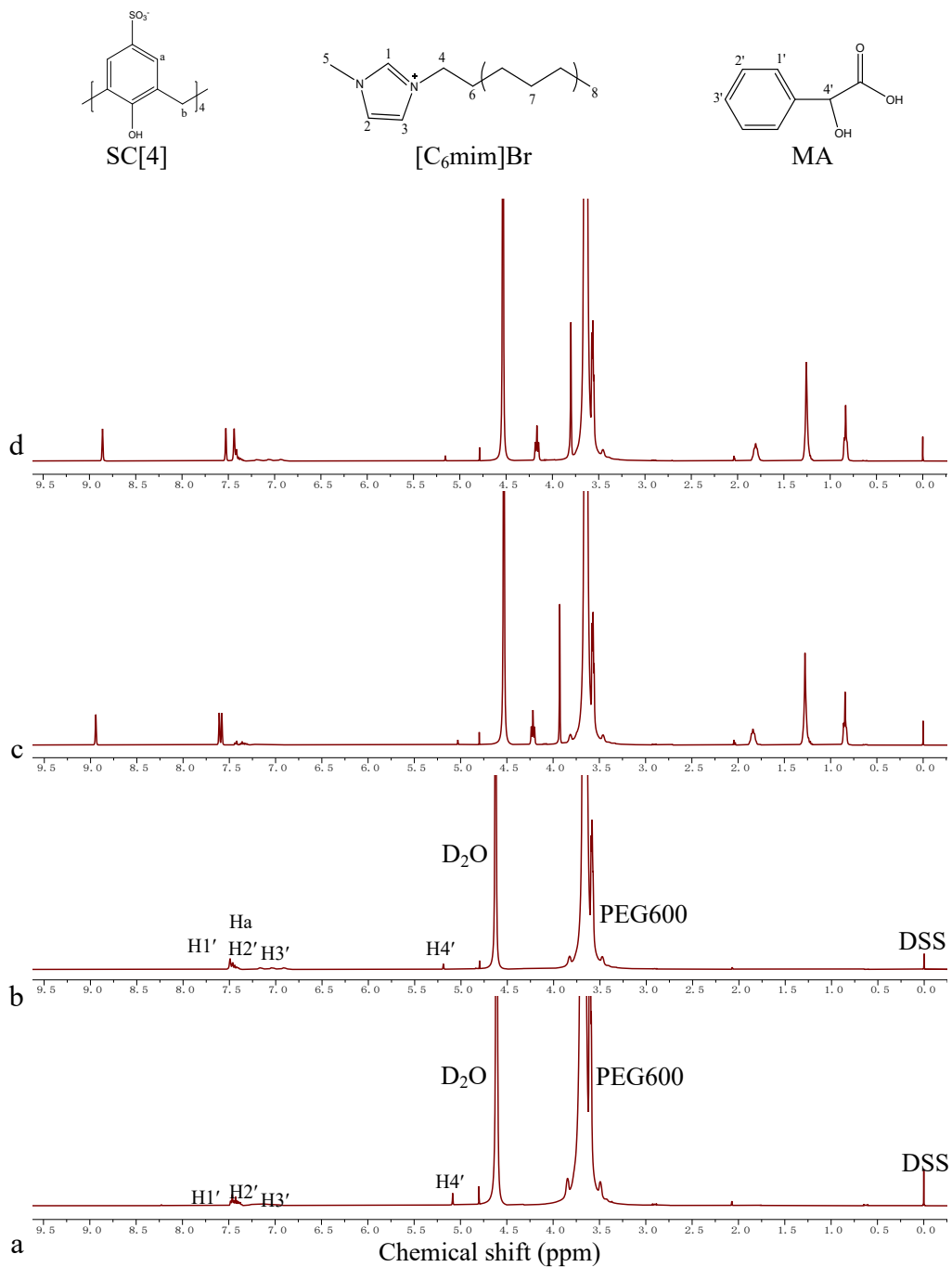


Fig. S6 The ¹H NMR spectra of the top phase of PEG 600 (25.0 wt%)/(NH₄)₂SO₄ (20.0 wt%)/MA ATPS in the absence (a) and presence (b-d) of an adjuvant. Adjuvant: SC[4] (1.0 wt%, b), [C₆mim]Br (5.0 wt%, c), and SC[4] (1.0 wt%)/[C₆mim]Br (5.0 wt%) (d).

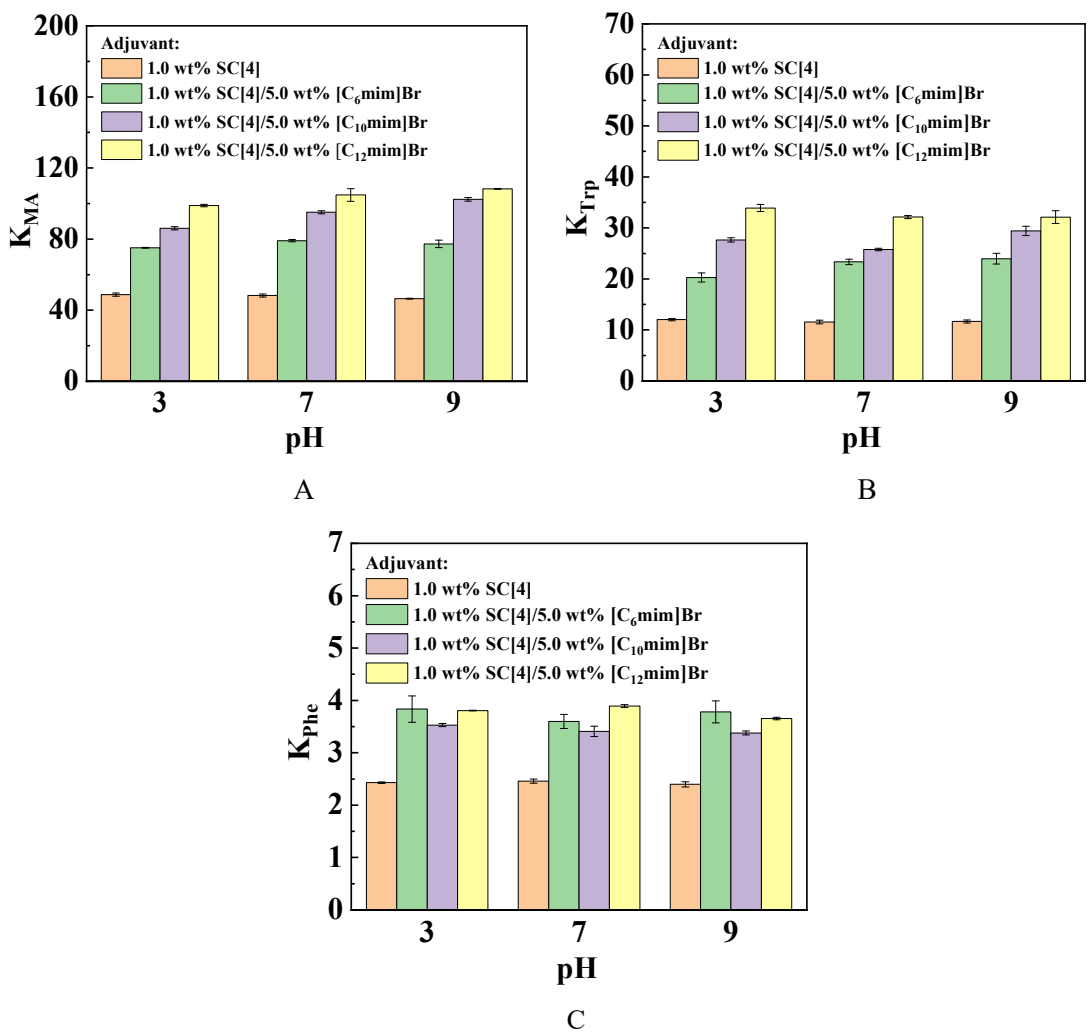


Fig. S7 The partition coefficients of MA (K_{MA}), Trp (K_{Trp}), and Phe (K_{Phe}) in PEG 600/(NH₄)₂SO₄/SC[4] (1.0 wt%)/[C_nmim]Br (5.0 wt%) ATPS at different pH values.

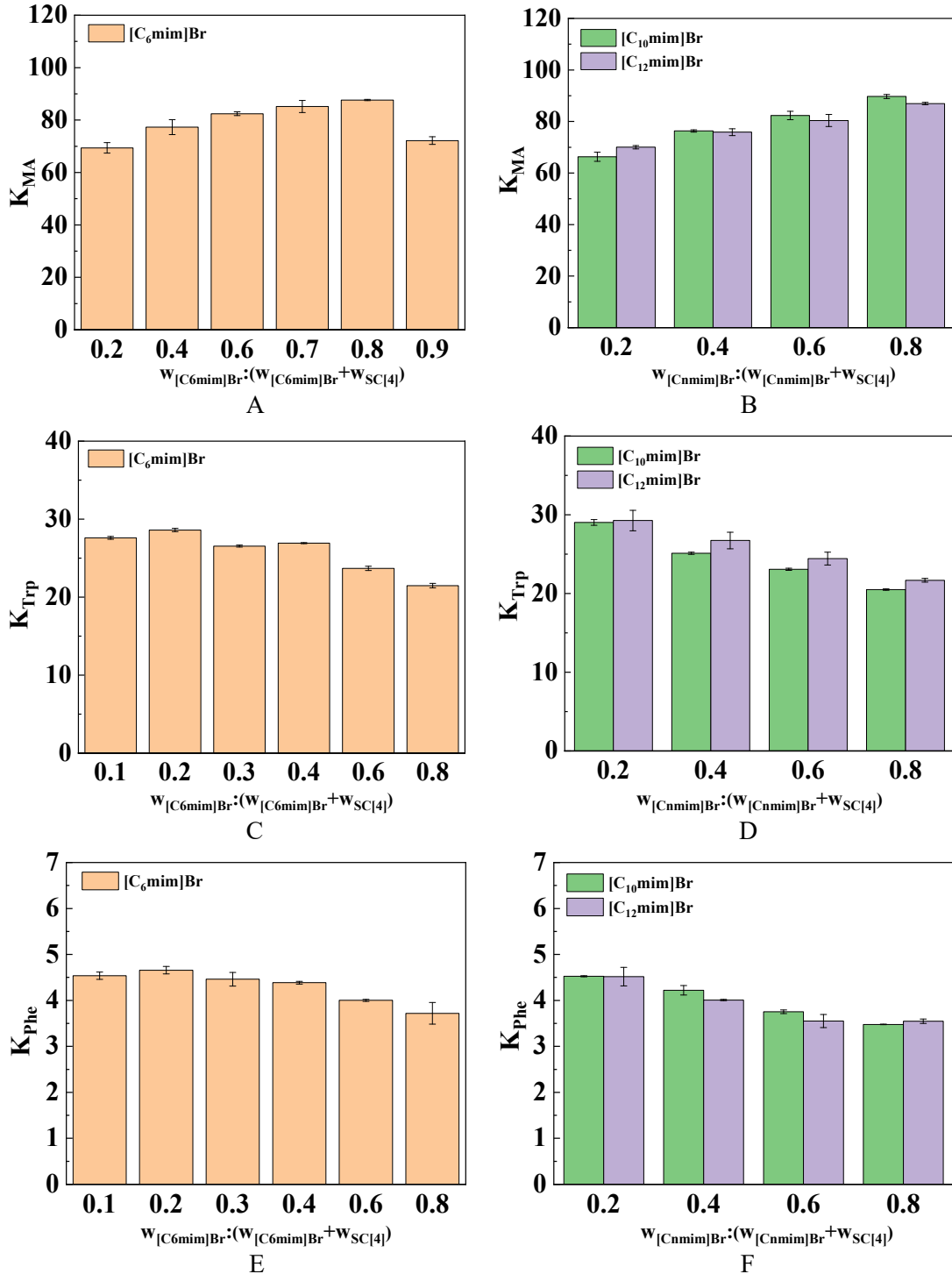


Fig. S8 The partition coefficients of MA, Trp, and Phe in PEG 600/ $(\text{NH}_4)_2\text{SO}_4/\text{SC}[4]/[\text{C}_n\text{mim}]Br$ ATPS at pH 7. The total weight of $[\text{C}_n\text{mim}]Br + \text{SC}[4]$ is 5.0 wt%.

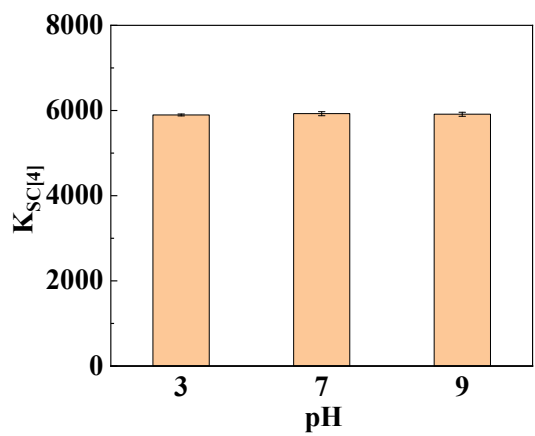


Fig. S9 Effect of pH on the partition coefficients of SC[4] (5.0 wt%) in PEG 600 (25.0 wt%)/(NH₄)₂SO₄ (20.0 wt%)/SC[4] (5.0 wt%) ATPS.